Int J Adv Manuf Technol (2013) 69:1079–1086
DOI 10.1007/s00170-013-5086-7

ORIGINAL ARTICLE

Optimization of loading path in hydroforming T-shape using fuzzy control algorithm

Bugang Teng · Kai Li · Shijian Yuan

Received: 18 February 2012 / Accepted: 24 May 2013 / Published online: 11 June 2013

Abstract The loading path is crucial to the quality of forming parts in the process of tube hydroforming, and thus the design and optimization of loading path is an important issue for tube hydroforming. Wrinkling is a catastrophic defect for thin-walled tube hydroforming. In order to avoid wrinkling, an adaptive simulation approach integrated with a fuzzy control algorithm is used to optimize the loading path of hydroforming a T-shaped tube. The tubular material used is stainless steel and has an outer diameter of 103 mm and the wall thickness of 1.5 mm. The controlled variables are the axial feeding, the counterpunch displacement, and the internal pressure. A code is developed to make the optimization automatically, which works together with LS-DYNA. Six evaluation functions are adopted for identifying geometrical shape and quality of T-shape. Failure indicators obtained from the simulation results are used as the input of the fuzzy control, and then process parameters are adjusted according to the expert experiences in the fuzzy controller. In this way, a reasonable loading path for producing a sound T-shape is obtained, and also a T-shaped product is successfully hydroformed by experiment. The result shows that the fuzzy control algorithm can provide an adequately reliable loading path for hydroforming T-shaped tubes.

Keywords T-shape · Hydroforming · Fuzzy control · Loading path · Optimization

1 Introduction

Manufacturing of complicated components with high quality induce that the hydroforming process is becoming one of the main interest for researchers and manufactures. The development of hydroforming technology has also led to a wide range of application in industry, especially for manufacturing high-quality lightweight components for the automobile, aviation, and aerospace industry [1–3]. Compared with conventional stamping and welding processes, the advantages of tube hydroforming include part consolidation on assemblies, weight reduction, improved structural strength and stiffness, excellent material utilization, fewer secondary operations, and improved part quality [4–7].

There are many different variables in this process that have significant influences on the final quality of products, hence, manufacturing of different components without any defects such as bursting or wrinkling encounters many difficulties. Currently, finite element simulation is generally used to reduce the product design time of hydroforming, and process design phases should also be expedited and shortened [8]. However, manufacturing engineers usually have to rely on their trial-and-error method in process design due to a lack of comprehensive system knowledge.

Many researchers have concentrated on the design and optimization of load paths in the hydroforming process. Ray et al. [9, 10] investigated the manufacturing of T- and X-shaped joints by using an intelligent load control algorithm, which can determine the optimal load paths for X- and T-branch tube hydroforming processes by maximizing the part expansion and simultaneously maintaining the wall thickness, forming stresses, and plastic strains within the allowable limits. Aydemir et al. [11] used ABAQUS and the fuzzy adaptive approach to simulate a T-shaped tube hydroforming process. The wrinkling and bursting criterion based on energy and the forming limit curve are, respectively, employed. However, in above works, load path of controlling the counterpunch for a branch was not considered. Imaninejad et al. [12] used LS-DYNA and the optimization software LS-OPT to optimize the internal pressure and axial feed loading paths for a T-joint design, in which the minimum thickness

B. Teng (✉) · K. Li · S. Yuan
National Key Laboratory for Precision Hot Processing of Metals, Harbin Institute of Technology, P.O. Box 435, 92 West Da-Zhi Street, Harbin 150001, China
e-mail: bgteng@hit.edu.cn

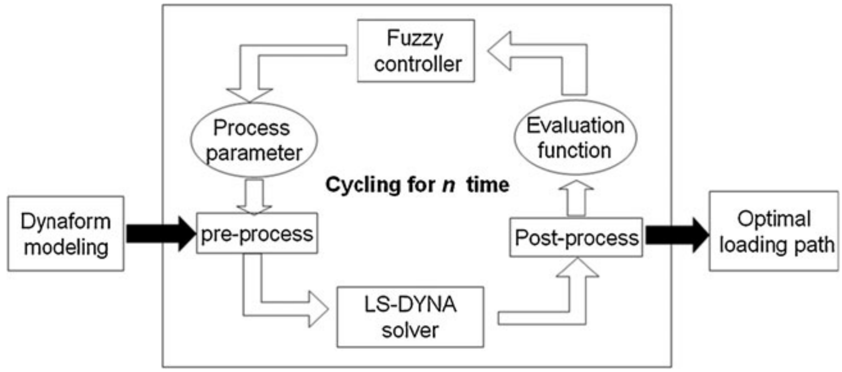

Fig. 1 Scheme of the adaptive simulation procedure

variation is chosen as the design objective, while keeping the maximum effective stress below the material ultimate strength. Jansson et al. [13] proposed an adaptive optimization method based on the use of response surface methods. The objective of the optimization is to maximize the minimum thickness, while keeping the maximum wrinkling at an acceptable level. Lorenzo et al. [14] developed a gradient-based approach to optimize the process of Y-shaped tube hydroforming, and both the internal pressure path and the counterpunch action were taken into account. Abedrabbo et al. [15] used genetic algorithm search method to optimize the process parameters and determine the best loading paths for tube hydroforming process, in which FLSD is chosen as the failure criterion. In addition, Mirzaali et al. [16] used simulated annealing optimization algorithm for optimizing internal hydraulic pressure to obtain the maximum formability of axisymmetric tubes under a failure criteria based on material's FLD. Manabe et al. [17] developed a fuzzy control system to optimize the loading conditions of hydroforming an aluminum alloy T-shaped tube with a counterpunch. Two evaluation functions are used for identifying geometrical shape and quality of T-shaped tube, i.e., wavy buckling deformation of the branch and the contact length between the counterpunch and the top of the branch.

This paper deals mainly with the effect of loading parameters on the T-shape hydroforming process. A fuzzy logic-based load control algorithm is developed for the control of the internal pressure and the axial feeding. An adaptive system is proposed to obtain adequate process parameters for hydroforming T-shaped tubes. Six evaluation functions are considered for identifying the geometrical shape and the quality of T-shaped tubes. The counterpunch control algorithm is also considered in this study. To demonstrate the effectiveness of this fuzzy adaptive process control system, experiments of hydroforming a stainless steel T-shape have been carried out. By comparing the experimental results with the simulated results, the validity of the fuzzy control system for hydroforming T-shaped tubes with a counterpunch is confirmed.

2 Adaptive simulation approach by using fuzzy control algorithm

In the process of hydroforming T-shaped tubes, there is normally a tendency of wrinkling, if the axial feeding is too large with respect to the applied internal pressure. On the other hand, if the internal pressure is too high with respect to the axial feeding, then there is a chance of bursting of the tube due to the excess wall thinning. Thus, the forming load parameters have to be properly adjusted and tuned in order to obtain a sound component. An adaptive approach is based on the ability to early detect the onset and growth of defects or

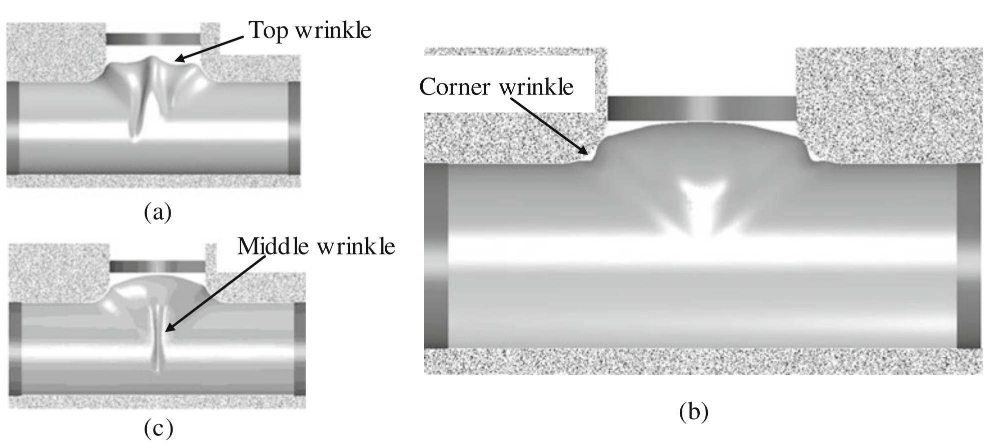

Fig. 2 Wrinkle location for hydroforming T-shapes due to unreasonable load path

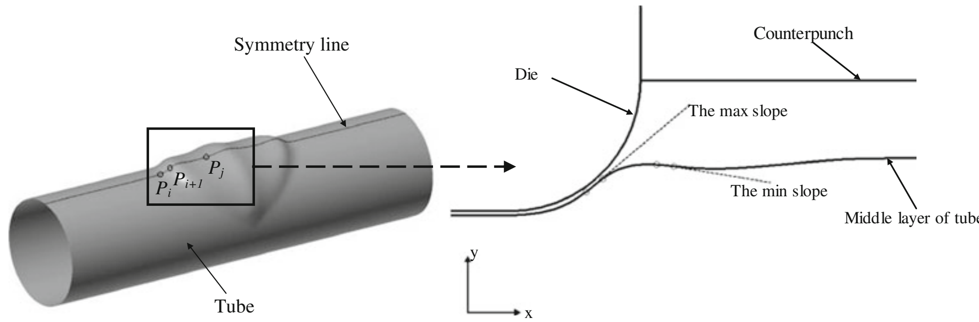

Fig. 3 Diagram of slope evaluation function

the occurrence of unwanted situations during the process and promptly react to them. In this work, winkling of the tube is considered as the main process failure criteria, and based on this failure criterion, the fuzzy adaptive process control is developed. The general strategy of the proposed method is that, under the condition of no wrinkling, as far as possible more axial feeding and less internal pressure will be provided to ensure the minimum thinning. The scheme of the adaptive simulation procedure is shown as Fig. 1.

The total simulation of the process is performed in many discrete steps simulations. In each step, the pressure, the axial feeding, and the counterpunch action are adjusted by the fuzzy load control algorithm as per requirement, which are calculated on the basis of values of evaluation functions. Evaluation functions are adopted for identifying current geometrical shape and quality of T-shape, and their values are processed into fuzzy language variables for fuzzy controller as input values. The process parameters of the next step are calculated by the optimized fuzzy control algorithm and are adjusted according to fuzzy control rules. Using these parameters, preprocess program rebuilds the finite element analysis (FEA) model and delivers the model to LS-DYNA solver. The load control algorithm acts as a closed-loop control system controlling the pressure, the axial feeding, and the counterpunch action to avoid wrinkling of the tube. The final optimal loading path is the superposition of the process parameters in each step. An adaptive system is developed to make the optimization automatically, which works together with LS-DYNA/explicit.

2.1 Evaluation functions

Wrinkling prediction in FEA is generally based on three main methods, i.e., plastic bifurcation theory, energy method, and geometry method. The geometry method is employed in this paper to indicate the onset of wrinkles.

There are several geometry-based wrinkles due to unreasonable load parameters during hydroforming T-shapes. Wrinkles usually encounter at the top of branch, the middle of main tube, and the corner between main tube and branch, which are illustrated in Fig. 2.

In the initial stage, excessive axial feeding can result in the wrinkle at the top of branch, as shown in Fig. 2a. This can be indicated through the slope variation of nodes of interest. Figure 3 is the schematic of the onset of wrinkles indicated by the slope variation. The slope k_{ij} are simply calculated from any two nodal coordinates between points i and j along the symmetry line.

$$k_{ij} = \left(y_i - y_j\right) \Big/ \left(x_i - x_j\right), i = 1, 2, \ldots, j-1; j = i, i+1, \ldots, n \tag{1}$$

where (x_i, y_i) is the nodal coordinates of point i along the symmetry line, and n is the number of node.

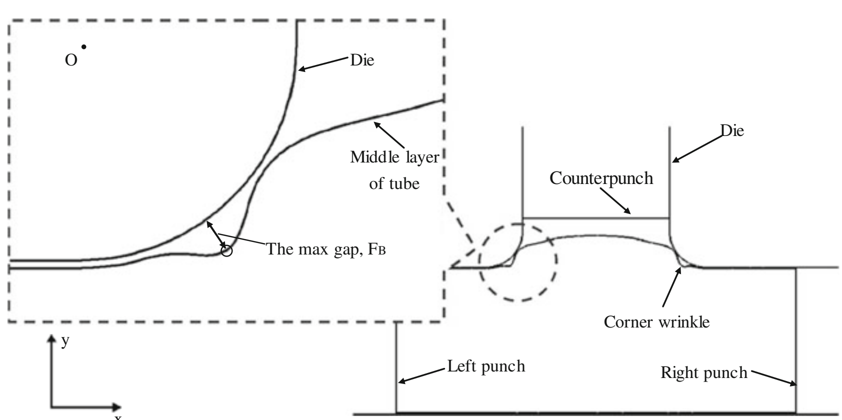

Fig. 4 Corner wrinkle in the transition zone

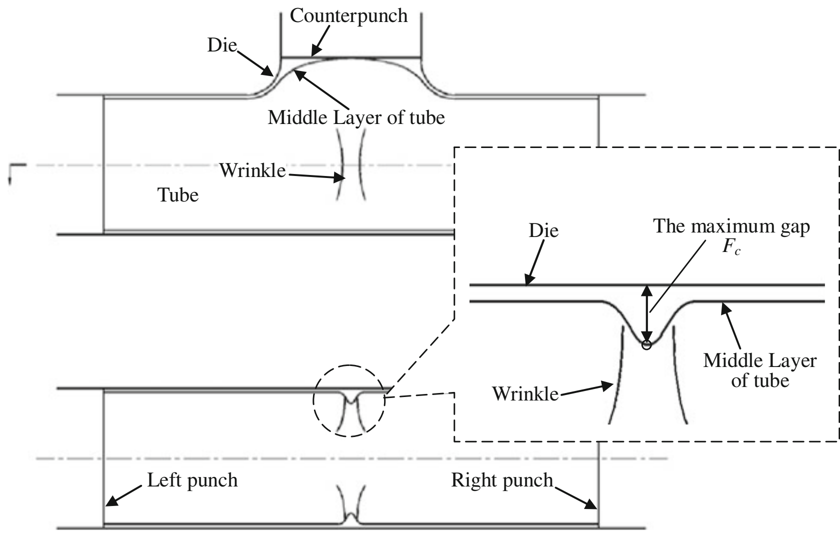

Fig. 5 Diagram of the evaluation function F_C for middle wrinkle

The maximum slope $F_{A\max}$ and the minimum one $F_{A\min}$ between any two nodes along the symmetry line can be defined as follows:

$$F_{A\max} = \max\{k_{12}, k_{13}, \ldots, k_{1n}, k_{23}, \ldots, k_{(n-1)n}\} \quad (2)$$

$$F_{A\min} = -\min\{k_{12}, k_{13}, \ldots, k_{1n}, k_{23}, \ldots, k_{(n-1)n}\} \quad (3)$$

The slope variation of the wrinkle-free part does not change the sign between positive and negative; whereas the sign will change during the onset of wrinkling. The changed sign of slope and the minimum slope $F_{A\min}$ can be used to indicate an existence of wrinkles in the forming process, and whether the wrinkle is an unstable folding due to the excessive axial feeding or the lower internal pressure.

Corner wrinkle between main tube and branch shown in Fig. 2b is another kind of defects in the T-shape forming process. The maximum gap F_B between tube and die along the symmetry line can be used to indicate the existence of wrinkles. It can be seen in Fig. 4.

F_B=max $\{d_1, d_2\ldots,d_1\}$, where d_i is the gap between die and any node in the corner region along the symmetry line.

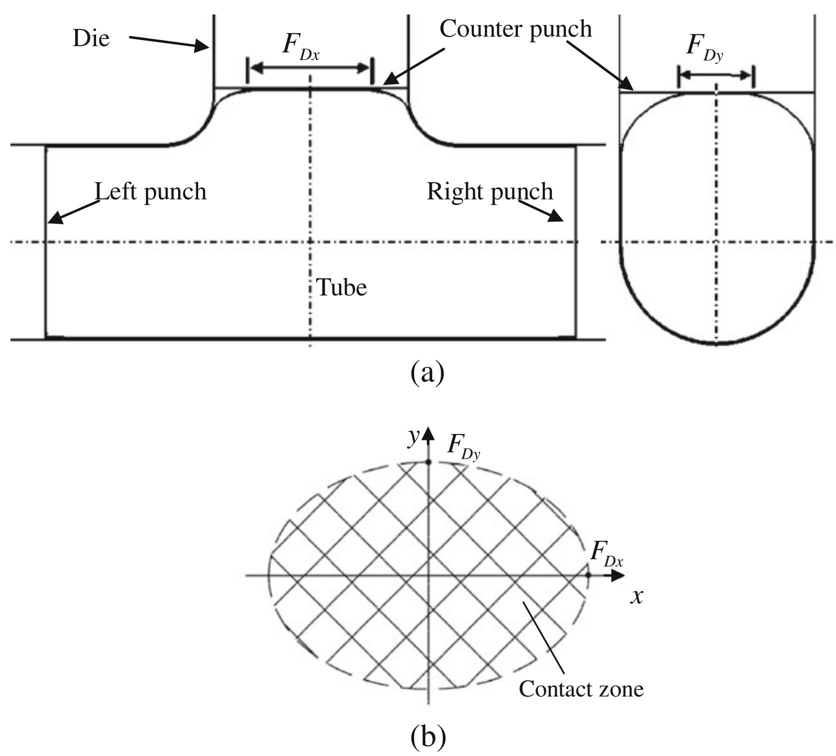

Fig. 6 Diagram of contact length evaluation functions (**a**) and diagram of the forming process (**b**). Contact zone between the branch and counterpunch

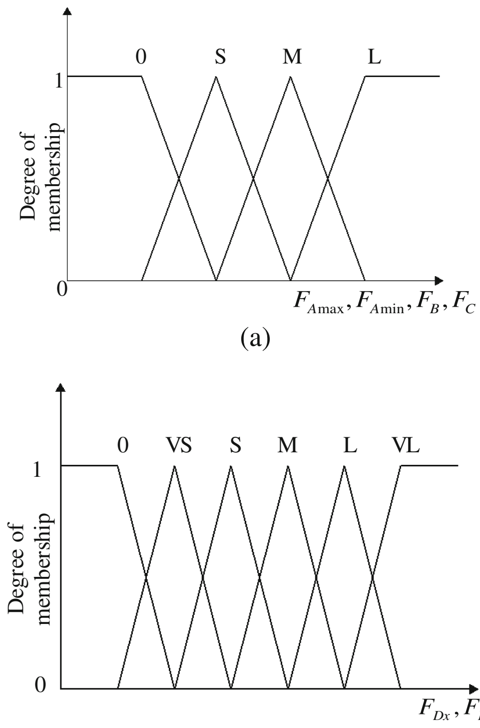

Fig. 7 Membership functions of input variables **a** $F_{A\max}$, $F_{A\min}$, F_B, F_C **b** F_{Dx}, and F_{Dy}

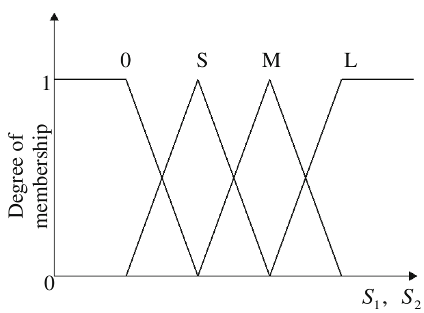

Fig. 8 Membership functions of output variables

Middle wrinkle shown in Fig. 2c can be detected by the maximum gap F_C between tube and die, as shown in Fig. 5, which is adopted as an evaluation function to measure this defect.

F_C=max$\{d_1, d_2…,d_1\}$, where d_i is the gap between any node of tube and side wall of the die.

The counterpunch imposing reaction force during the process is an effective method to avoid excessive thinning of formed branch. Figure 6 is the scheme of the branch contacting with the counterpunch during forming process, it can be seen that the contact length is varied in different contact direction. The contact zone shown in Fig. 6b is an approximate ellipse, and the length of major axis F_{Dx} and the length of minor axis F_{Dy} are adopted as evaluation functions to measure the area of the contact zone.

Table 2 Mechanical properties of tube used from uniaxial tensile test

σ_s (MPa)	σ_b (MPa)	n	K(MPa)	r	v	δ(%)
325	637	0.385	1173	0.8	0.28	49.5

2.2 Design of fuzzy algorithm controller

The geometry of interest location of T-shape during forming can be described by the values of these six evaluation functions mentioned above, i.e., the maximum and minimum slope $F_{A\max}$ and $F_{A\min}$, the maximum gap F_B and F_C, the length of major and minor axis of contact ellipse F_{Dx} and F_{Dy}. In this paper, the fuzzy algorithm controller is developed to decide hydroforming parameters according to the different status of the tube. The values of evaluation functions should be fuzzed as the input variables of the controller. The evaluation functions $F_{A\max}$, $F_{A\min}$, F_B, and F_C are fuzzed into four sets (zero, small, medium, and large), whose membership functions are shown in Fig. 7a. Similarly, F_{Dx} and F_{Dy} are fuzzed into six sets (zero, very small, small, medium, large, and very large), whose membership functions are shown in Fig. 7b.

Similarly, the output variables of the fuzzy controller for the axial feeding S_1 and the counterpunch displacement S_2 were divided into four sets, i.e., zero, small, medium, and large. The membership functions are shown in Fig. 8.

In this adaptive simulation system, T-shape hydroforming process was divided into three stages (initial, middle, and final stages) in order to simplify the fuzzy control rules. In the initial stage, the counter punch is fixed, while the axial punches impose the axial feed, and the liquid pressure is added into the tube at a fast speed simultaneously. At this stage, the protrusion dose not contact with the counter punch, it is in free-bulging state. In the initial stage, $F_{A\max}$, $F_{A\min}$, F_B, and F_C are considered as the input variables in the fuzzy control of the axial feeding. Because each evolution function has four sets (zero, small, medium, and large), 256 combinations should be considered by the axial feeding fuzzy

Table 1 Chemical composition of the 1Cr18Ni9Ti (China)

Element	C	Si	Mn	S	P	Cr	Ni	Ti
Wt.%	0.037	0.56	1.51	0.0019	0.028	17.23	9.57	0.5

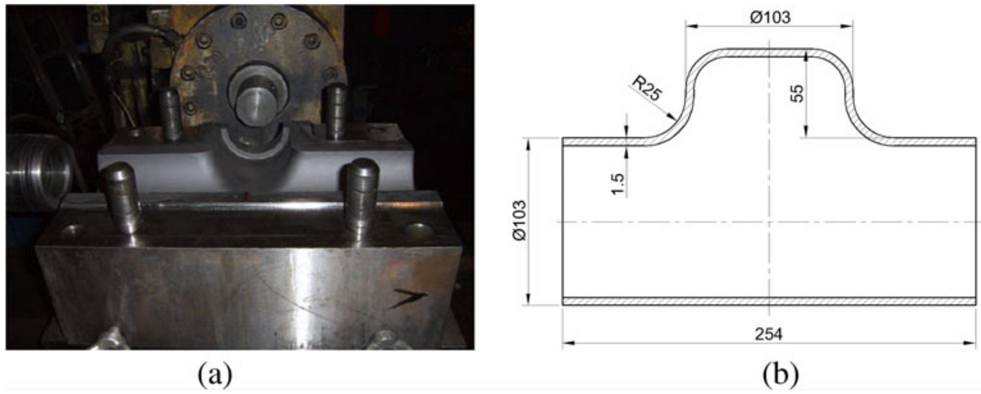

Fig. 9 Tool and shape of the product. **a** The lower die and **b** dimension of the tube product

control rules in this stage. The middle stage of forming starts from the time of contact between the top of the protrusion and the counter punch to the time of basic affixation. In the final stage, the counter punch begins to retract, but maintains contact with the top of the protrusion, and imposes counter punch force on top of the protrusion to avoid excessive thinning at the top of the protrusion. In the middle and final stage, F_{Dx}, F_{Dy}, F_B, and F_C are regarded as the input variables for the counterpunch displacement fuzzy control, and F_B and F_C are used as the input variables in the fuzzy control of the axial feeding. Evolution function F_{Dx} and F_{Dy} are fuzzed into six sets (zero, very small, small, medium, large, and very large). So in the middle and final stage, 576 combinations should be considered by the counterpunch displacement fuzzy control rules and also 16 combinations by the axial feeding fuzzy control rules.

So a total of 848 fuzzy control rules with different combination of evaluation functions are used to decide axial feeding and counterpunch displacement. For example, for the control of the axial feeding, If $F_{A\max}$ is L (large), $F_{A\min}$ is 0(zero), F_B is 0(zero), F_C is 0(zero), then axial feeding is L (large). The fuzzy control rule of the counterpunch displacement can be expressed if F_{Dx} is VL (very large), F_{Dy} is S (small), F_B is 0 (zero), F_C is 0 (zero), then the counterpunch displacement is S (small).

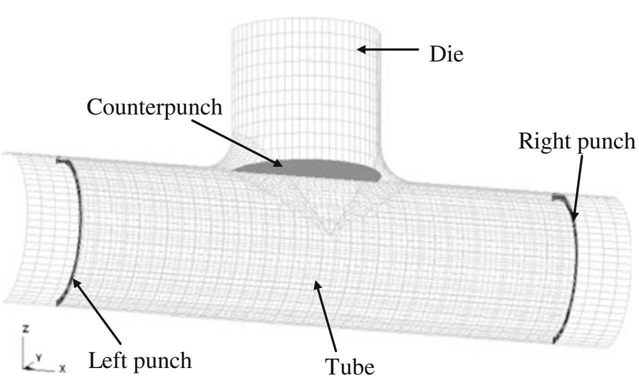

Fig. 10 The FEM model of T-shape hydroforming

3 Adaptive simulation and experiment of T-shaped tube hydroforming

To confirm the validity of adaptive simulation system based on the fuzzy control algorithm for T-shaped tube hydroforming, the adaptive simulation and experiment have been carried out. The tube material is 1Cr18Ni9Ti (China); to determine the mechanical properties of the tube, tensile specimens are cut from the tube and tested. The chemical composition and material properties of the 1Cr18Ni9Ti stainless steel are presented in Tables 1 and 2, respectively.

The special hydroforming press is used for T-shape hydroforming. This hydroforming press consists of a hydraulic press for closing the die, three horizontal cylinders, a pressure intensifier, a hydraulic drive system, and a computer control system. The major parameters are the maximum internal pressure 400 MPa, the closing force 3,150 kN, the left and right horizontal axial force 800 kN, and the middle horizontal axial force 500 kN, which provided the support for the counterpunch. Figure 9 presents the lower die used for experiment and the dimension of the T-shape to be formed.

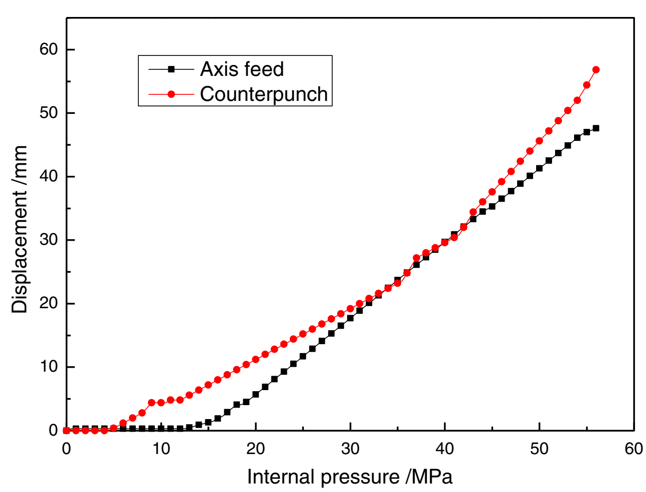

Fig. 11 Optimized loading curve from adaptive simulation

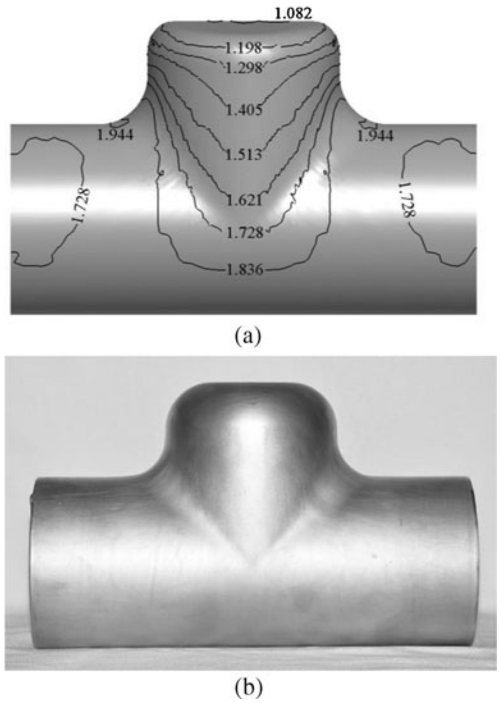

Fig. 12 Results of **a** adaptive simulation and **b** experiment

3.1 FEM model

An adaptive simulation code based upon fuzzy control algorithm and evaluation functions mentioned above was developed to optimize loading path for T-shape hydroforming. Working together with LS-DYNA, the software can automatically design optimized loading path instead of traditional trail-and-error FEA approach. Wrinkle indicators obtained from the simulation results are used as the input of the fuzzy control, and then process parameters are adjusted according to the expert experiences in the fuzzy controller.

A blank tube with outer diameter of 103 mm, initial length of 340 mm, and wall thickness of 1.5 mm is used. The diameter of the branch tube is equal to that of the main tube, and the radius between main tube and the branch is 25 mm. The initial distance between the counterpunch and the tube is 0 mm. The lubricant is formulated with MoS_2 (spray type) and is applied to the die and outer tube surface.

In the FE model, only half part of the tube is actually analyzed due to the symmetry of the problem, as shown in Fig. 10. The tube is discreted to BT shell elements; the number of elements is 3,400, all of which are quadrilateral elements. The die is discreted to rigid elements; the total amount is 1,984; 1,835 of which are quadrilateral elements, and 149 of which are triangular elements. The leftward and rightward punches are discreted to rigid elements; there are 324 elements, 312 of which are quadrilateral elements, and 12 are triangular elements. The counter punch is also discreted to rigid elements, there are 1,077 of them, 1,040 of which are quadrilateral elements, and 37 are triangle elements.

In the simulation, the work hardening law of material is $\sigma = K\varepsilon^n$. Strength coefficient value K=1,173 and work hardening exponent n=0.385, which is obtained from uniaxial tensile test. Other parameters are: density 7.83 g/cm^3, Young's modulus 207GPa, Poisson's ratio 0.28. Contact between the tube and die is modeled using a penalty-based contact algorithm, and the friction coefficient of 0.05 is applied to the contact surface. Pressurized liquid is imposed by uniform pressure, which is added on the internal face of the tube.

The adaptive simulation parameters are set as follows: final branch height is 55 mm, final top radius of the branch

Fig. 13 The thickness distribution of formed tube

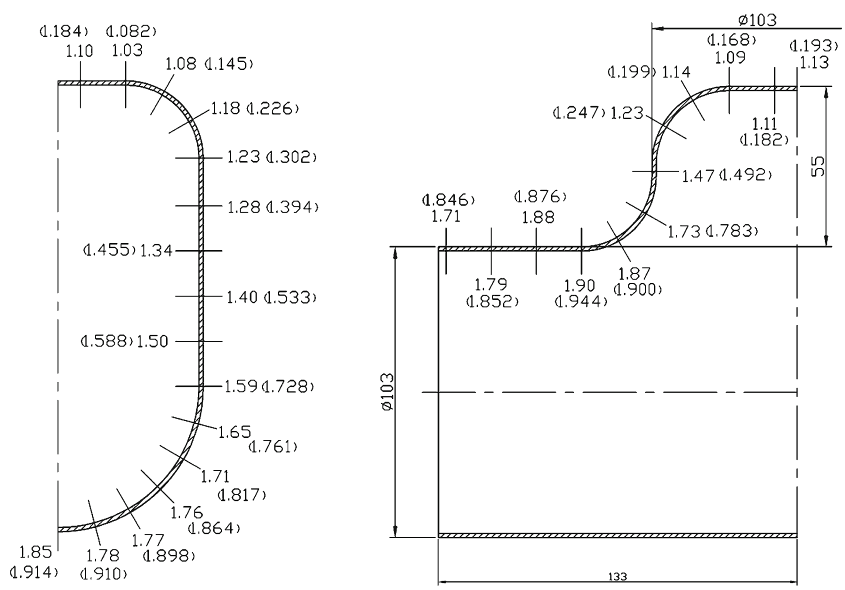

is less than 15 mm, and the internal pressure increment for each loop is 0.5 MPa.

3.2 Adaptive simulation and experimental results

The computation is performed using a low-cost PC (Pentium 4, 2.40 GHz, 512 MB RAM) running Windows XP. After 112 times loop of adaptive simulation, which costs about 31 h, the program ended normally, and the requirement of tube shape was satisfied. The process parameters of every single-step are calculated by the optimized fuzzy control algorithm, which is adjusted according to the expert experience. The final optimized loading path is the superposition of every single step. The optimized loading curve shown in Fig. 11 is generated by the adaptive simulation using the fuzzy control algorithm. The final internal pressure is 56 MPa, and the final axial feeding is 47.6 mm (unilateral). The simulation result of tube wall thickness distribution is shown in Fig. 12a, which indicated that the minimum thickness at the top corner of branch tube is 1.08 mm (the thinning rate 28 %), and the maximum thickness at the transition region between the main and branch tube is 1.94 mm (the thickening rate 29.3 %). The experiment of T-shape hydroforming using the optimized loading curve generated by the adaptive simulation is carried out, and the experimental result is shown in Fig. 12b.

The experimental product is cut linearly along axial direction to measure thickness at the designated points (see Fig. 13). The values in brackets are simulation results. The minimum thickness at the top corner of branch tube is 1.03 mm (the thinning rate 31.3 %), the error is 3.3 % compared with the adaptive simulation result. The maximum thickness at the rounded transition region between the main and branch tube is 1.90 mm (the thickening rate 26.7 %), which is less than 2.6 % compared with the adaptive simulation one.

4 Conclusion

A T-shape hydroforming adaptive simulation system, worked together with LS-DYNA, based on the fuzzy control algorithm is developed in this paper. Six evaluation functions are used to identify geometrical shape of forming tube and to indicate the onset of wrinkling. The adaptive system can generate the optimized loading curve automatically, and a stainless steel thin-walled T-shaped product was successfully hydroformed using the optimized loading path, which was obtained from this system. The experimental result shows that the maximum thinning and the thickening ratio of the T-shape are 31.3 and 26.7 %, respectively. Comparing with the simulation results, the error of the maximum or minimum thickness is less than 3.3 %. Experimental results confirm the validity of the fuzzy control system for hydroforming T-shapes with a counterpunch.

Acknowledgments This work was financially supported by the National Key Technology R&D Program, Development of Advanced Forming Technologies of High Strength Steel and Integration Applications in Target Car, and the National Natural Science Foundation of China (project number: 50875060). The authors would like to take this opportunity to express their sincere appreciation.

References

1. Dohmann F, Hartl C (1997) Tube hydroforming—research and practical application. J Mater Process Technol 71:174–186
2. Yuan SJ, Lang LH, Wang XS, Wang ZR (2001) Experimental and numerical simulation of aluminum tube hydroforming, in: Proceedings of the Second International Conference on Hydroforming, Fellbach, Germany, pp 339-347
3. Li B, Nye TJ, Metzger DR (2006) Multiobjective optimization of forming parameters for tube hydroforming process based on the Taguchi method. Int J Adv Manuf Technol 28:23–30
4. Yuan SJ, Liu G, Huang XR, Wang XS (2004) Hydroforming of typical hollow components. J Mater Process Technol 151:203–207
5. Koc M, Altan T (2001) An overall review of the tube hydroforming (THF) technology. J Mater Process Technol 108:384–393
6. Jirathearanat S, Hartl C, Altan T (2004) Hydroforming of Y-shapes product and process design using FEA simulation and experiments. J Mater Process Technol 146:124–129
7. Cheng DM, Teng BG, Guo B, Yuan SJ (2009) Thickness distribution of a hydroformed Y-shape tube. Mater Sci Eng A 499:36–39
8. Kwan CT, Lin FC (2003) Investigation of T-Shape tube hydroforming with finite element method. Int J Adv Manuf Technol 21:420–425
9. Ray P, Mac Donald BJ (2004) Determination of the optimal load path for tube hydroforming processes using a fuzzy load control algorithm and finite element analysis. Finite Elem Anal Des 41:173–192
10. Ray P, Mac Donald BJ (2005) Experimental study and finite element analysis of simple X- and T-branch tube hydroforming processes. Int J Mech Sci 192:1498–1518
11. Aydemir A, Vree JHP, Brekelmans WAM (2005) An adaptive simulation approach designed for tube hydroforming processes. J Mater Process Technol 159:303–310
12. Imaninejad M, Subhash G, Loukus A (2006) Loading path optimization of tube hydroforming process. Int J Mach Tool Manuf 45:1504–1514
13. Jansson M, Nilsson L, Simonsson K (2007) On process parameter estimation for the tube hydroforming process. J Mater Process Technol 190:1–11
14. Lorenzo RD, Ingarao G, Chinesta F (2009) A gradient-based decomposition approach to optimize pressure path and counterpunch action in Y-shaped tube hydroforming operations. Int J Adv Manuf Technol 44:49–60
15. Abedrabbo N, Worswick M, Mayer R (2009) Optimization methods for the tube hydroforming process applied to advanced high strength steels with experimental verification. J Mater Process Technol 209:110–123
16. Muzaalia M, Liaghata GH, Naeini HM (2011) Optimization of tube hydroforming process using simulated annealing algorithm. Procedia Eng 10:3012–3019
17. Manabe K, Suetake M, Koyama H, Yang M (2006) Hydroforming process optimization of aluminum alloy tube using intelligent control technique. Int J Mach Tool Manuf 46:1207–1211